Ground-level ozone in four Chinese cities: precursors, regional transport and heterogeneous processes

L. K. Xue[1,2*], T. Wang[1,2,3*], J. Gao[3], A. J. Ding[4], X. H. Zhou[2], D. R. Blake[5], X. F. Wang[2], S. M. Saunders[6], S. J. Fan[7], H. C. Zuo[8], Q. Z. Zhang[2], and W. X. Wang[2,3]

[1]Department of Civil and Environmental Engineering, Hong Kong Polytechnic University, Hong Kong, China

[2]Environment Research Institute, Shandong University, Ji'nan, Shandong, China

[3]Chinese Research Academy of Environmental Sciences, Beijing, China

[4]Institute for Climate and Global Change Research and School of Atmospheric Sciences, Nanjing University, Nanjing, Jiangsu, China

[5]Department of Chemistry, University of California at Irvine, Irvine, CA, USA

[6]School of Chemistry and Biochemistry, University of Western Australia, WA, Australia

[7]College of Environmental Science and Engineering, Sun Yat-Sen University, Guangzhou, Guangdong, China

[8]College of Atmospheric Sciences, Lanzhou University, Lanzhou, Gansu, China

[*]*To whom correspondence should be addressed*

E-mail: cetwang@polyu.edu.hk and xuelikun@gmail.com*, Tel: +852-2766 6059, Fax: +852-2330 9071*

Abstract.

We analyzed the measurements of ozone (O_3) and its precursors made at rural/suburban sites downwind of four large Chinese cities – Beijing, Shanghai, Guangzhou and Lanzhou, to elucidate their pollution characteristics, regional transport, *in-situ* production, and impacts of heterogeneous processes. The same measurement techniques and observation-based model were used to minimize uncertainties in comparison of the results due to difference in methodologies. All four cities suffered from serious O_3 pollution but showed different precursor distributions. The model-calculated *in-situ* O_3 production rates were compared with the observed change rates to infer the relative contributions of on-site photochemistry and transport. At the rural site downwind of Beijing, export of the well-processed urban plumes contributed to the extremely high O_3 levels (up to an hourly value of 286 ppbv), while the O_3 pollution observed at suburban sites of Shanghai, Guangzhou and Lanzhou was dominated by intense *in-situ* production. The O_3 production was in a VOCs-limited regime in both Shanghai and Guangzhou, and a NO_x-limited regime in Lanzhou. The key VOC precursors are aromatics and alkenes in Shanghai, and aromatics in Guangzhou. The potential impacts on O_3 production of several heterogeneous processes, namely, hydrolysis of dinitrogen pentoxide (N_2O_5), uptake of hydro peroxy radical (HO_2) on particles and surface reactions of NO_2 forming nitrous acid (HONO), were assessed. The analyses indicate the varying and considerable impacts of these processes in different areas of China depending on the atmospheric abundances of aerosol and NO_x, and suggest the urgent need to better understand these processes and represent them in photochemical models.

1 Introduction

Air quality in the metropolitan areas has drawn increasing attention in recent years (Molina and Molina, 2004; Parrish and Zhu, 2009). A typical and difficult issue is photochemical smog characterized by unhealthily high concentrations of ground-level ozone (O_3), which is a product of atmospheric photochemistry involving nitrogen oxides (NO_x=NO+NO_2) and volatile organic compounds (VOCs). The ozone problem is a complex coupling of primary emissions, chemical transformation, and dynamic transport at different scales (Jacob, 1999). Challenges in regulating O_3 pollution primarily lie in understanding its non-linear chemistry with respect to precursors (i.e., NO_x, CO and VOCs) and contributions from both local and regional sources.

China has become home to several megacities and many large cities owing to its fast-paced

urban-industrialization processes. It is not surprising that these cities have been experiencing air quality deterioration in light of their fast expansion in economics, energy use and motor vehicles in the past decades. High O_3 concentrations exceeding the national ambient air quality standards have been observed frequently in and downwind of large cities (e.g., Wang et al., 2006, 2010b; Zhang J. et al., 2007; Zhang Y. et al., 2008; Ran et al., 2009; Chou et al., 2011). Recent studies also indicated increasing O_3 trends in several highly urbanized regions, i.e., the North China Plain (NCP; 1995–2005, Ding et al., 2008; 2005–2011, Zhang et al., 2014), Yangtze River delta (YRD; 1991–2006, Xu et al., 2008) and Pearl River delta (PRD; 1994–2007, Wang et al., 2009b). Furthermore, a worsening prospect of the problem is even foreseen in view of the projected continuing increase in emissions of NO_x and VOCs in the near future (Ohara et al., 2007). Consequently, effective control strategies based on scientifically sound knowledge must be in place in order to return to the clearer and cleaner skies.

Atmospheric models are the common tools used to understand the O_3 formation processes. The chemical mechanisms underlying the models are usually simplified representations of the complex atmospheric chemistry, with the organic species of similar reactivities and structures grouped into one model species (Stockwell et al., 2012). This chemical lumping gives reduced computational runtimes, but may produce extra uncertainties when applied to different atmospheric conditions (e.g., with different VOC emissions; the lumped mechanisms are usually optimized with emission estimates in some developed regions). The Master Chemical Mechanism (MCM) is a nearly-explicit mechanism that has the minimum amount of chemical lumping (Jenkin et al., 2003; Saunders et al., 2003), and hence is the best choice to investigate atmospheric photochemistry for a variety of environments. Another source of uncertainty is heterogeneous chemical processes which have recently been found to be more complex than previously thought. Several cases in point are the hydrolysis of dinitrogen pentoxide (N_2O_5), uptake of hydro peroxy radical (HO_2) on particles, and surface reactions of NO_2 forming nitrous acid (HONO) (Brown et al., 2006; Thornton et al., 2008; Su et al., 2011). These processes are believed to be more relevant in China given its very high aerosol loadings. However, they are usually neglected by most of the current mechanisms (such as MCM), and to date only very limited studies have attempted to evaluate their potential impacts and suggested the important role of HO_2 uptake in O_3 formation (e.g., Kanaya et al., 2009; Liu et al., 2012).

Another challenge in understanding ground-level O_3 problem is to dissect the local and regional contributions. Two types of methods have been widely used for this. One is the chemical transport model that is ideal to quantify local and regional contributions but may be subject to uncertainties from the emission inventory estimates (Wang et al., 2010c; Tie et al., 2013). The other approach is observation-based and usually comprises concurrent measurements from at least a pair of stations (Wang et al., 2010b; Berlin et al., 2013). It assumes that the O_3 concentrations at the upwind site can be regarded as the regional background for the receptor site. To our knowledge, there are very limited studies that estimated the contributions of local production and regional transport based on the observations at a single locale (e.g., Frost et al., 1998).

To evaluate the atmospheric impacts of emerging Chinese megacities, intensive observations of O_3 and O_3 precursors were conducted from 2004 to 2006 in suburban/rural areas near four Chinese major cities, namely Beijing, Shanghai, Guangzhou, and Lanzhou. These cities are located in different regions of China (see Fig. 1) and have different geographies, climates, industries and emission patterns. The same measurement techniques were utilized in all campaigns to minimize uncertainties arising from experiments in comparison of the results. These studies generated much high-quality data in the mid-2000s in major urban areas of China, which will be invaluable for assessing the atmospheric impact of on-going rapid urbanization in China. For data analysis, an observation-based MCM model (OBM) was deployed to quantify the contributions of *in-situ* photochemistry and regional transport and to assess the potential impacts of several heterogeneous processes. Overall, this study reveals the similarly serious O_3 pollution, different distributions in O_3 precursors, and varying impacts of heterogeneous chemistry in major cities of China.

2 Methodology

2.1 Study areas and sites

The field experiments were conducted in rural/suburban areas near three megacities in Northern (Beijing), Eastern (Shanghai) and Southern (Guangzhou) China, and a large city in Western China (Lanzhou; see Fig. 1). The sampling sites were selected carefully downwind of city centers during the study periods to allow investigation of regional-scale pollution and processes. These sites have been described separately by Wang et al. (2006); Gao et al. (2009); Zhang et al. (2009a) and Pathak et al. (2009), and here we only give a brief outline.

Beijing is the capital city of China and among the largest cities in the world. It is located on the northwestern periphery of the densely-populated North China Plain, and accommodates more than 19 million inhabitants, 5 million automobiles, and dozens of factories and power plants. The observations were carried out from 21 June to 31 July 2005 in a rural mountainous area in Chang Ping district (CP; 40°21' N, 116°18' E, 280 m a.s.l.), about 50 km north (generally downwind in summer) of the downtown. The site was in a fruit farm with sparse population and anthropogenic emissions about 10 km away (Wang et al., 2006). The rural nature of the site determines to a large extent the 'unique' results obtained in Beijing (i.e., highest O_3, lowest O_3 precursors, and dominant role of regional transport) compared to the other three cities (suburban sites), which should be kept in mind when comparing the results among the four sites.

Shanghai is the largest city of China and located in the Yangtze River Delta. It has over 23 million population, 2 million vehicles, China's largest petrochemical complex, steel manufacturer, seaport and other industries. The study site was in the Taicang Meteorological Station (31°27' N, 121°06' E, 20 m a.g.l.), which is approximately 45 km northwest of Shanghai. Although Taicang belongs to Jiangsu Province, it is often affected by urban plumes of Shanghai under the prevailing southeasterly winds in the summer-monsoon season. The observations taken from 4 May to 1 June 2005 were analyzed in the present study.

Guangzhou is a megacity of over 12 million people in southern China. It is in the center of the Pearl River Delta, which has been a 'world factory' for a wide range of consumer products. The measurements were made at Wan Qing Sha (WQS; 22°42' N, 113°33' E, 17 m a.g.l.), a suburban area about 50 km southeast of downtown Guangzhou. The data collected between 20 April and 26 May 2004 were analyzed in this paper. Thus the present study targets the O_3 pollution in late spring, and can be compared with and supplement previous investigations that focused on autumn (Zhang J. et al., 2007; Zhang Y. et al., 2008).

Lanzhou is a large city of over 3 million people and an industrial center in the interior western China. It is situated in a narrow valley basin in a mountainous region with a mean altitude of 1520 m a.s.l. This unique topography, together with its petrochemical industry as well as vehicle emissions (0.2 million cars in 2006), makes it a typical 'basin' of O_3 pollution in summer (Zhang et al., 2000). The sampling site was located in Renshoushan Park (RSP; 36°8' N, 103°41' E), a suburban mountainous area with some peach trees and other vegetation (Zhang et al., 2009a). The

industrial zone (Xigu petrochemical district) is located about 5 km to the southwest, and the urban center is about 15 km to the southeast. The intensive campaign was conducted from 19 June to 16 July 2006.

2.2 Measurement techniques

The same set of techniques were deployed to measure O_3, CO, SO_2, NO, NO_y, VOCs, particle number and size distribution, and meteorological parameters at the four cities. O_3 was monitored by a UV photometric instrument (*Thermo Environmental Instruments (TEI), Model 49i*). CO was measured by a non-dispersive infrared analyzer (*Advanced Pollution Instrumentation, Model 300EU*) with internal zeroing automatically done every 2 hours. SO_2 was observed with a pulsed UV fluorescence analyzer (*TEI Model 43c*). NO and NO_y were detected by a chemiluminescence analyzer (*TEI Model 42cy*) coupled with an external molybdenum oxide catalytic converter to reduce NO_y to NO (Xue et al., 2011). Aerosol number and size distribution (10 nm – 10 μm) were measured in real-time under ambient humidity conditions by a Wide-range Particle Spectrometer (*MSP, WPS model 1000XP*) in Beijing, Shanghai and Lanzhou. Temperature, pressure, relative humidity (RH), wind direction and speed, and solar radiation were continuously measured by a weather station. All the above measurement techniques and quality assurance/control procedures have been described elsewhere (Gao et al., 2009; Xue et al., 2011).

Methane and C_2-C_{10} non-methane hydrocarbons (NMHCs) were measured by collecting whole air samples in evacuated stainless-steel canisters with subsequent analysis by gas chromatography with flame ionization detection, electron capture detection, and mass spectrometry (the analysis was undertaken in the University of California at Irvine) (Xue et al., 2013). Generally, one sample was collected at noon each day during the field campaigns (note that the sampling was not made consecutively at Lanzhou). In addition, multiple samples were taken on selected ozone episode days, normally one sample every two hours from 7:00 to 19:00 LT. Such a sampling strategy aimed at facilitating both a thorough evaluation of VOC pollution for the campaigns and a comprehensive modeling analysis for the high O_3 events. In total, 130, 68, 76, and 24 VOC samples were collected in Beijing, Shanghai, Guangzhou, and Lanzhou, respectively.

2.3 Observation-based model

An observation-based chemical box model was utilized to quantify the *in-situ* O_3 production.

The model has been successfully applied in the previous studies (Xue et al., 2013, 2014a and 2014b). Briefly, it is built on the Master Chemical Mechanism (v3.2), a nearly-explicit mechanism describing oxidation of 143 primary VOCs together with the latest IUPAC inorganic nomenclature (Jenkin et al., 2003; Saunders et al., 2003). In addition, heterogeneous processes including uptake of N_2O_5, NO_3 and HO_2 on aerosols and reactions of NO_2 on ground/particle surfaces producing HONO are also incorporated (see details in Section 3.4). Dry depositions of inorganic gases, peroxides, PANs, carbonyls and organic acids are adopted in the model from the recent compilation (Zhang et al., 2003). The mixing-layer height affecting dry deposition rates was assumed to vary from 300 m at night to 1500 m in the afternoon. Sensitivity model runs with other maximum mixing heights (i.e., 1000 and 2000 m) showed that its impact on the modeling results was negligible (i.e., <3% in net O_3 production rates).

The observed data of O_3, CO, SO_2, NO, CH_4, C_2-C_{10} NMHCs, H_2O, temperature, pressure, and aerosol surface and radius were averaged or interpolated with a time resolution of 1-hour and used as the model inputs. The aerosol surface and radius were calculated from the aerosol number and size distribution measurements. For Guangzhou where such measurements were not available, we used the average diurnal data obtained from a similar suburban site in Hong Kong (Tung Chung, close to the WQS site; see Fig. S1) in the same season (May 2012). Sensitivity studies using 50% higher aerosol surface indicated little impact on the modeling results (i.e., ~1% in net O_3 production rate). For hydrocarbons for which the observations were not in real-time, the time-dependent concentrations at hourly resolution were estimated as follows. During the daytime (i.e., 7:00-19:00) when multiple samples were taken, the data gaps were filled by time interpolation. The nighttime concentrations were estimated based on the regressions with CO (for most hydrocarbons except for isoprene) and temperature (for isoprene), for which continuous measurements were available. Photolysis frequencies were computed as a function of solar zenith angle (Saunders et al., 2003), and were further scaled by the measured solar radiation. The model calculations were made for the identified O_3 episode days with 00:00 LT as the initial time. Before each simulation, the model pre-ran for nine days with constraints of the campaign-average data so that the model approached a steady state for the unmeasured species (e.g., NO_2 and radicals).

The model read the inputs every hour to calculate the *in-situ* O_3 production and destruction rates. The ozone production rates calculated by the OBM usually correspond to the production of total

oxidant (O_x=O_3+NO_2) other than O_3 alone (by considering the oxidation of NO to NO_2 by peroxy radicals; Kanaya et al., 2009; Xue et al., 2013). Here we determined directly the reaction rates of O_3 instead of O_x with our model. In the troposphere, O_3 production is eventually achieved by the combination of O atom with O_2 (*R1*), and O_3 destruction is mainly facilitated by O_3 photolysis (*R2*) and reactions with NO (*R3*), NO_2 (*R4*), OH (*R5*), HO_2 (*R6*), atoms of O (*R7*) and Cl (*R8*), and unsaturated VOCs (*R9*) (In general, the O_3 destruction was dominated by reactions of R2-R4, while the other reactions may also make considerable contributions at specific conditions (e.g., at high VOCs).

$$O_2 + O + M \rightarrow O_3 + M \quad (R1)$$

$$O_3 + h\nu \rightarrow O(^1D) + O_2 \quad (R2a)$$

$$O_3 + h\nu \rightarrow O + O_2 \quad (R2b)$$

$$O_3 + NO \rightarrow NO_2 + O_2 \quad (R3)$$

$$O_3 + NO_2 \rightarrow NO_3 + O_2 \quad (R4)$$

$$OH + O_3 \rightarrow HO_2 + O_2 \quad (R5)$$

$$HO_2 + O_3 \rightarrow OH + 2O_2 \quad (R6)$$

$$O_3 + O \rightarrow O_2 + O_2 \quad (R7)$$

$$O_3 + Cl \rightarrow ClO + O_2 \quad (R8)$$

$$O_3 + \textit{unsat.}\ \text{VOCs} \rightarrow \text{carbonyls} + \text{Criegee biradical} \quad (R9)$$

Thus the O_3 production and destruction rates can be calculated as:

$$P(O_3) = k_1[O_2][O][M] \quad (E1)$$ (M denotes N_2 or O_2)

$$L(O_3) = J_{O3}[O_3] + k_3[NO][O_3] + k_4[NO_2][O_3] + k_5[OH][O_3] + k_6[HO_2][O_3] + k_7[O][O_3] + k_8[Cl][O_3] + \sum(k_{9i}[VOC_i])[O_3] \quad (E2)$$

Then the net O_3 production rate can be determined from the difference between $P(O_3)$ and $L(O_3)$. We also compared our-derived O_3 net rates with those of O_x from the traditional method, and found both methods showed overall good agreement (see Fig. S2).

3 Results and discussion

3.1 Overview of O_3 and O_3 precursors

Table 1 summarizes the overall O_3 pollution conditions observed in the four cities. At the rural

site of Beijing, eighteen O_3 episode days (here defined as days when the peak hourly O_3 exceeded 100 ppbv; 44% of the total) were observed during the 6-week measurement period. The maximum hourly O_3 mixing ratio was 286 ppbv, which is by far the highest value reported in China in open literatures (Wang et al., 2006). Such frequency of episodes and extreme O_3 levels highlight the serious problem in the Beijing area. At the suburban site near Shanghai, six episode days (21%) occurred during the 4-week campaign with the maximum hourly O_3 of 127 ppbv observed. The pollution in Shanghai (YRD) seemed relatively lighter than those in other three cities, which may be due to the titration effect of its high NO_x levels (Ding et al., 2013). At the downwind site of Guangzhou, seven episodes (19%) were encountered throughout the 37 measurement days. The maximum hourly O_3 concentration was recorded at 178 ppbv. This indicates that the O_3 pollution in the PRD is serious not only in autumn but also in late spring. In Lanzhou, eight episodes (29%) took place during the 4-week campaign with a maximum hourly O_3 of 143 ppbv. Our observations highlight the serious ozone pollution in the large cities of China.

We then examined the distributions of major O_3 precursors observed in the four cities. The mean diurnal profiles of NO_y and CO are shown in Figure 2. At the rural site of Beijing with little local emissions, both precursors showed high levels in the late afternoon till the evening, corresponding to regional transport of urban plumes. At the suburban sites downwind of Shanghai, Guangzhou and Lanzhou, in comparison, they exhibited a morning maximum and/or another evening peak, which were mainly caused by the shallow boundary layer and enhanced emissions in the rush hours. The NO_y levels measured in Shanghai (24–39 ppbv) and Guangzhou (24–52 ppbv) were significantly higher than those in Beijing (rural site; 11–16 ppbv) and Lanzhou (7–27 ppbv), while the CO levels were comparable in the four cities despite the relatively lower afternoon concentrations in Lanzhou.

Figure 3 documents the average reactivities towards OH of major hydrocarbons in the four cities (see Supplement for the OH reactivity calculation). To facilitate interpretation of the hydrocarbon speciation, the 50+ species were categorized into anthropogenic hydrocarbons (AHC; encompassing most species except for isoprene and α/β-pinenes) and biogenic hydrocarbons (BHC; comprising isoprene and α/β-pinenes), with AHC further grouped into reactive aromatics (R-AROM; including all aromatics except for benzene), alkenes, alkanes with ≥4 carbons (C4HC), and low-reactivity hydrocarbons (LRHC; including methane, ethane, propane, acetylene and benzene; see in Table S1). The highest hydrocarbon reactivity was determined in Lanzhou (9.33 s^{-1} in total), followed by those

in Shanghai (5.85 s^{-1}) and Guangzhou (5.23 s^{-1}). This is opposite to the patterns for NO_y and CO as shown in Fig. 2. The lowest reactivity (2.77 s^{-1}) was measured at the Beijing site, which should be ascribed to the fact that our site is located in a rural mountainous area with few local anthropogenic emissions. It also implies that the urban plumes had undergone extensive photochemical processing during transport and were less reactive when reaching the Beijing site.

Furthermore, different hydrocarbon distributions among the four cities were also illustrated. In Beijing and Shanghai, the AHC reactivities were dominated by both alkenes (35% and 43%) and R-AROM (34% and 39%). In Guangzhou, R-AROM was the dominant AHC class with an average contribution of 46%. And in Lanzhou, alkenes played a predominant role and composed on average 70% of the AHC reactivity. In particular, the propene and ethene levels were extremely high, both of which contributed 53% of the AHC reactivity. These results suggest distinct emission patterns of O_3 precursors and imply different O_3 formation regimes in the four cities (see next section).

3.2 Process analysis: regional transport vs. *in-situ* formation

To understand the processes contributing to high O_3 pollution in the four cities, we analyzed in detail twelve O_3 episodes (3 per city; Beijing: 9, 26, 30 July 2005; Shanghai: 7, 8, 22 May 2005; Guangzhou: 18, 23, 24 May 2004; Lanzhou: 5, 11, 12 July 2006). These cases were chosen because elevated O_3 levels were observed and the most comprehensive measurements (i.e., multiple daily VOC samples) were made. (The time series of O_3 and related parameters during these episodes are shown in Figures S3-S6.) At a given location, the change of O_3 mixing ratios is a combined result of *in-situ* photochemistry, regional transport (both horizontal and vertical) and deposition. The contributions of chemistry and transport can be either positive (i.e., production and import) or negative (i.e., destruction and export). In the present study, we examined the contributions of *in-situ* photochemistry and regional transport to the observed O_3 pollution by using observations coupled with OBM analysis. We first determined the rate of change in O_3 concentrations from the observed O_3 time series (R_{meas}). The *in-situ* net O_3 production (R_{chem}) and deposition rates (R_{deps}) were computed every hour by the OBM as described in Section 2.3. Then the difference ($R_{trans} = R_{meas} - R_{chem} - R_{deps}$) can be considered as the contribution from regional transport (note that the effect of atmospheric mixing was also included in this term).

Figure 4 displays the time series of O_3 and contributions of *in-situ* production, deposition and regional transport for typical O_3 episodes at the four cities (the results were similar for other cases

for each city and are not shown). Two interesting phenomena are illustrated. One is the intrusion of residual boundary-layer air contributing to O_3 increase during the early morning period. At all four cities, in particular Lanzhou, R_{trans} presented an important contributor to the O_3 increase in the early morning. This should be attributed to mixing with the O_3-rich air aloft when the nocturnal boundary layer is broken down. The other is the sudden changes of the transport effect corresponding to the variation in surface winds. During the Beijing case (Fig. 4a), for example, the southeasterly winds brought urban plume to the study site, resulting in an O_3 peak at 14:00–15:00; but after that the wind direction shifted to northerly, leading to a sharp O_3 decrease. Similar wind effects were also noticed for the Guangzhou and Lanzhou cases. These results suggest that our method can capture the variations in physical processes and hence is capable of quantifying the contributions of regional transport.

We are particularly interested in the relative roles of *in-situ* photochemistry and transport in the extremely high O_3 levels observed at the rural site downwind of Beijing. As shown in Figure 4a, both *in-situ* production and regional transport contributed to the O_3 accumulation from morning (~40 ppbv at 8:00 LT) to noon (~100 ppbv at 12:00 LT). In the afternoon, however, the O_3 mixing ratios increased sharply from ~100 ppbv to ~220 ppbv within less than two hours (14:00-15:00 LT), during which the *in-situ* O_3 production had been weakened due to the relatively low levels of VOCs and NO_x. Thus such a sharp O_3 rise was attributed to the transport of urban plumes from Beijing that had undergone extensive photochemical processing and contained high amounts of produced O_3. This is a very typical case at CP in summer, and highlights the efficient export of Beijing urban pollution in the afternoon, which can adversely affect the vegetation and crops in downwind areas.

In comparison, the *in-situ* production dominated the O_3 accumulation throughout the daytime at suburban sites downwind of Shanghai, Guangzhou and Lanzhou (see Figures 4b-d). Very strong O_3 formation was determined during these episodes (e.g., up to 50, 90 and 40 ppbv/h at Shanghai, Guangzhou and Lanzhou). Regional transport generally made a negative contribution (i.e., export) to the observed O_3 pollution. This indicates that the air masses at these sites were reactive enough to sustain the observed O_3 increase and even had potential to export the produced O_3 to downwind regions.

We then examined the ozone formation regimes in Shanghai, Guangzhou and Lanzhou, where *in-situ* photochemistry dominated the O_3 pollution, by calculating the relative incremental reactivity

(RIR) with the OBM. RIR is defined as the ratio of decrease in O_3 production rate to decrease in precursor concentrations, and can be used as a metric for the effect of a given emission reduction on O_3 concentrations (Cardelino and Chameides, 1995). The daytime-average RIRs for major groups of O_3 precursors during the episodes are shown in Fig. 5. Overall, the O_3 formation regimes were consistent among cases for each city but different among cities. In Shanghai and Guangzhou, the *in-situ* O_3 production was highly VOC-sensitive, specifically AHC-controlled (see Fig. 5a). The RIRs for NO_x were negative. Within the AHC dominated were reactive aromatics and alkenes in Shanghai and aromatics in Guangzhou (see Fig. 5b). This suggests that reducing emissions of aromatics (and also alkenes for Shanghai) would weaken the O_3 formation in both cities, yet cutting NO_x emissions may aggravate the local O_3 problems.

In Lanzhou, the O_3 formation was most sensitive to NO_x and to a lesser extent to AHC. Within the AHC, alkenes were the most important compounds responsible for the O_3 production. In particular, light olefins such as propene and ethene were the most abundant reactive species, both of which presented approximately half of the AHC reactivity (figure not shown). Such high levels of olefins are attributable to the industrial structure of Lanzhou, which is a well-known petrochemical city in West China with the China National Petroleum Corporation – Lanzhou Petrochemical Company and many small petrochemical plants located in its Xigu district. Light olefins are major components of the petrochemical plant emissions (Ryerson et al., 2003). The results suggest that the most efficient way to alleviate the O_3 pollution in Lanzhou is to cut the NO_x emissions (from petrochemical and power plants as well as vehicles), while reducing emissions of olefins (from the petrochemical plants) could also result in considerable decrease in O_3 formation.

3.3 Impact of heterogeneous processes

In this section, we assess the potential impacts of several poorly-understood heterogeneous processes on the ozone production in the four target cities, by incorporating them in the OBM and conducting sensitivity analyses.

3.3.1 $ClNO_2$ production from N_2O_5 hydrolysis

The hydrolysis of N_2O_5 may produce nitryl chloride ($ClNO_2$), which is usually accumulated at night and can enhance the next-day's O_3 formation by releasing both NO_2 and chlorine atom (it can oxidize hydrocarbons like OH) via photolysis. The hydrolysis rate is considered to be first order of

the N_2O_5 concentrations (Chang et al., 2011). This process has not been considered by most of the current mechanisms (e.g., MCM), and is here parameterized in our MCM-based model as follows.

$$N_2O_5 \rightarrow (2\text{-}\emptyset) * NO_3^- + \emptyset * ClNO_2 \qquad k_{10} \qquad (R10)$$

Where, ϕ is the production yield of $ClNO_2$, and k_{10} is the first order rate constant and estimated by

$$k_{10} = \frac{1}{4} \times v_{N2O5} \times \gamma_{N2O5} \times S_{aero} \qquad (E3)$$

Where v_{N2O5} is the mean molecular speed of N_2O_5 and can be calculated from the gas kinetic theory (Aldener et al., 2006); γ_{N2O5} is the reactive uptake coefficient of N_2O_5 on aerosol surfaces; S_{aero} is the aerosol surface area concentration and is calculated based on the measured particle number size distributions. The current uncertainty of this process primarily lies in the uptake coefficient of N_2O_5 and production yield of $ClNO_2$, which are highly variable and dependent on the aerosol composition, humidity and temperature (Chang et al., 2011). The γ_{N2O5} derived on real atmospheric particles from limited available field observations were in the range of 0-0.04 (Chang et al., 2011, and references therein). In the present study, we adopted a moderate value of γ_{N2O5} = 0.03 with no production of $ClNO_2$ (ϕ = 0) in the base model, and conducted sensitivity analyses by including $ClNO_2$ production with a moderate yield of 60%.

Figure 6 illustrates the impacts of $ClNO_2$ formation from N_2O_5 hydrolysis on the O_3 production during the selected episodes in the four cities. Overall, the $ClNO_2$ produced/accumulated at night may enhance considerably the next-day's O_3 formation, and this impact is highly dependent on the abundances of both aerosol surface density (more interface) and nitrogen oxides (more reactants). For instance, including the $ClNO_2$ formation would result in an average nighttime $ClNO_2$ peak of 1.3 ppbv at the Shanghai site with high concentrations of both NO_x and particle surface, which in turn would enhance the daytime-average O_3 production rates by ~3 ppb/h on average (or 14% in percentage; the enhancement was the most significant in the early morning with the maximum percentage of ~26%, and then decreased over the course of the day). In comparison, this process seems to be less significant (<10% for the daytime-average) at the other three sites due to their relatively lower levels of NO_x and/or aerosol surface. It is noteworthy that the OBM cannot take into account the transport of $ClNO_2$ that has relatively long lifetime at night. $ClNO_2$ may present a positive altitude profile in the nocturnal boundary layer due to less O_3 titration above the ground. Intrusion of the air aloft in the early morning might contribute considerably to the $ClNO_2$ at surface

sites. Therefore, our estimation of the impact of $ClNO_2$ in the present study should be a lower limit. Nonetheless, our results indicate that the nighttime heterogeneous process of N_2O_5 is a considerable uncertainty in the current understanding of O_3 photochemistry in the high-NO_x and high-aerosol environments such as Shanghai. Clearly, *in-situ* measurements of N_2O_5 and $ClNO_2$ are urgently required to better understand this process and to provide more realistic parameterizations of γ_{N2O5} and ϕ_{ClNO2} which can be adopted in air quality models.

3.3.2 Uptake of HO_2 by aerosols

The heterogeneous loss of HO_2 on aerosol surface can act as an efficient radical sink at high aerosol loadings and thus attenuate O_3 production (Kanaya et al., 2009). This process is also usually ignored by the current mechanisms, and here was included in our model by adding the following reaction.

$$HO_2 \rightarrow \text{products} \qquad k_{11} \qquad (R11)$$

The reaction rates were assumed to be first order in the HO_2 concentrations. k_{11} is the reaction constant that can be calculated by

$$k_{11} = -\left(\frac{r}{D_g} + \frac{4}{\gamma_{HO2} \times v_{HO2}}\right)^{-1} S_{aero} \qquad (E4)$$

Where r is the surface-weighted particle radius; Dg is the gas phase diffusion coefficient and is assumed to be 0.247 $cm^2\ s^{-1}$ (Mozurkewich et al., 1987) (the gas diffusion limitation is accounted for here given the potential larger uptake of HO_2 to aerosol; see below); γ_{HO2} is the uptake coefficient of HO_2 on particles; v_{HO2} is the mean molecular speed of HO_2; and S_{aero} is the aerosol surface density. Similar to N_2O_5 hydrolysis, the uptake coefficient (γ_{HO2}) is a parameter with large uncertainty and is related to the aerosol composition, temperature and RH (Thornton et al., 2008). The laboratory studies determined the γ_{HO2} in the range of 0.01-0.2 for different types of non-metal aerosols at room temperatures, with much higher values (>0.2) measured on the Cu-doped aqueous surfaces (Mao et al., 2010, and references therein). Taketani et al. (2012) recently reported relatively large γ_{HO2} values for ambient aerosols at Mt. Tai (0.13-0.34) and Mt. Mang (0.09-0.40) in China. Here we adopted a value of γ_{HO2} = 0.02 in the base model, and changed it to an upper limit (0.4) for sensitivity model runs.

Figure 7 elucidates the effects of heterogeneous HO_2 loss on the modeled HO_2 concentrations

and O_3 production rates during episodes in the four cities. Varying impacts of this process in different cities are clearly illustrated. These impacts mainly depend on the abundances of aerosol surface, and are also related to the levels of nitrogen oxides (*i.e.*, at high-NO_x conditions, the HO_2 loss is dominated by its reactions with NO_x and its heterogeneous loss is less important) as well as the O_3 formation regimes (*i.e.*, the same HO_2 reduction would lead to less reduction in O_3 formation at NO_x-limited regime than at the VOCs-limited regime). At the Shanghai, Guangzhou and Lanzhou sites with relatively higher levels of NO_x or lower loadings of aerosols, adopting a higher uptake coefficient (γ_{HO2} = 0.4) would only lead to little to moderate reductions in the HO_2 concentrations (<21%) and O_3 production rates (<10%). At the Beijing site, however, a faster uptake would reduce significantly the HO_2 levels by about 50% due to its very high loadings of aerosol surface (~1600 $\mu m^2/cm^3$). Such HO_2 reduction would in turn result in an average decrease of ~15% in the daytime-average O_3 production rates (note that a relatively smaller reduction in O_3 production should be attributed to the more NO_x-sensitive O_3 production regime at our rural site). This indicates that the uptake of HO_2 presents another large source of uncertainty in current studies of O_3 photochemistry in the high-aerosol environments like Beijing, and more observational studies are required to quantify the γ_{HO2} on the real particles.

3.3.3 Surface reactions of NO_2 forming HONO

HONO is a key reservoir of the hydroxyl radical (OH) and hence plays a crucial role in atmospheric chemistry. Recent studies have indicated possible existence of 'missing' source(s) for daytime HONO, which cannot be reproduced by current models only considering the homogeneous source from the OH+NO reaction (e.g., Su et al., 2008 and 2011). It has been suggested that the photo-enhanced heterogeneous reactions of NO_2 on various surfaces should be an important source of HONO (Su et al., 2008; Li et al., 2010). In the present study, HONO was not measured but simulated within the model. In addition to the homogeneous source, heterogeneous sources from reactions of NO_2 on the ground and aerosol surfaces were also taken into account in the base model by adopting the parameterizations used by Li et al. (2010). The reaction rates were assumed to be first order of the NO_2 concentrations (Aumont et al., 2003), and the processes were simplified as follows.

$$NO_2 \rightarrow HONO \qquad kg \qquad (R12)$$

$$NO_2 \rightarrow HONO \qquad ka \qquad (R13)$$

kg and *ka* are the first order rate constants for the ground and aerosol surface reactions, and can be estimated as

$$k_g = \frac{1}{8} \times v_{NO2} \times \gamma_g \times \left(\frac{S}{V}\right) \qquad (E5)$$

$$k_a = \frac{1}{4} \times v_{NO2} \times \gamma_a \times S_{aero} \qquad (E6)$$

Where v_{NO2} is the mean molecular speed of NO_2; γ_g and γ_a are the uptake coefficients of NO_2 on the ground and aerosol surfaces; S/V is the effective surface density of the ground, and S_{aero} is the aerosol surface area concentration. Considering the photo-enhanced production of HONO from the surface reactions (George, 2005; Monge et al., 2010), higher values of γ_g and γ_a were used during the daytime than at night. For γ_g, we used a value of $\gamma_g = 1\times10^{-6}$ at nighttime, and increased it to 2×10^{-5} during the daytime with solar radiation smaller than 400 W/m^2. With more intense solar radiation, a higher γ_g value of $2\times10^{-5}\times$(solar radiation/400) was used (Li et al., 2010). As to γ_a, we used a value of $\gamma_a = 1\times10^{-6}$ at nighttime and increased it to 5×10^{-6} during the day, according to Li et al. (2010). An effective surface area of 1.7 m^2 per geometric ground surface was used to calculate the S/V (Vogel et al., 2003).

The heterogeneous HONO formation may enhance O_3 production by releasing OH via HONO photolysis. We conducted sensitivity model runs by turning off the heterogeneous HONO sources, which is the case of most current atmospheric models. The results are shown in Fig. 8. We can see that including these processes would enhance the daytime-average O_3 production rates by ~6.8 ppb/h and ~3.2 ppb/h on average (~25% and ~16%) in Shanghai and Guangzhou respectively, but lead to little change for the Beijing and Lanzhou sites (<1%). This corresponds well to the distributions of nitrogen oxides observed at the four sites (see Fig. 2). And aerosol surface loading seems not a key factor here, which is in line with the fact that the heterogeneous HONO formation on the ground generally dominates than those on the aerosol at the ground level (Su et al., 2008). These results suggest that the heterogeneous processes of NO_2 may play an important role in atmospheric photochemistry in the high-NO_x environments such as Shanghai and Guangzhou, and need to be included in the air quality models.

In-situ measurements of HONO, which were not available in China until recent years, have shown surprisingly elevated concentrations of HONO (up to the ppb level) throughout the daytime in the PRD region (e.g., Su et al., 2008). Such high levels of daytime HONO cannot be explained

by only including the above heterogeneous reactions of NO_2, and some additional sources have been proposed (e.g., Su et al., 2011). It is not known if this phenomenon was also the case at our study sites, however identification of additional HONO source(s) is beyond scope of the present study. The analyses presented here clearly indicate that the surface reactions of NO_2 at least present an important HONO source and can enhance O_3 production. Undoubtedly, *in-situ* measurements of HONO are critical for better understanding the atmospheric photochemistry including O_3 formation, and further efforts are needed to determine the 'missing' source(s).

4 Summary

Measurements of O_3 and O_3 precursors were made at a rural site downwind of Beijing and suburban sites of Shanghai, Guangzhou and Lanzhou. The data were analyzed to elucidate the O_3 precursor distributions, roles of transport and *in-situ* production, and impacts of heterogeneous processes. The major findings are summarized as follows.

(1) The four cities suffered from severe O_3 pollution and showed different precursor distributions. The NO_y levels in Shanghai and Guangzhou were higher than that in Lanzhou, while an opposite pattern was found for the VOC reactivity. The dominant anthropogenic hydrocarbons were alkenes in Lanzhou, aromatics in Guangzhou, and both alkenes and aromatics in Beijing and Shanghai.

(2) Transport of 'aged' urban plumes resulted in the extremely high O_3 levels (up to 286 ppbv) at the rural site downwind of Beijing, while intense *in-situ* photochemical production dominated at the suburban sites of Shanghai, Guangzhou and Lanzhou. The O_3 production was VOCs-limited in Shanghai and Guangzhou and NO_x-limited in Lanzhou. The key VOC species were aromatics and alkenes in Shanghai and aromatics in Guangzhou.

(3) The potential impacts of several poorly-understood heterogeneous processes on O_3 production were assessed. The N_2O_5 hydrolysis was more significant at the Shanghai site due to its high levels of both aerosol and NO_x. The HO_2 loss on aerosols was more relevant for Beijing because of its very high aerosol loadings. The HONO formation from surface reactions of NO_2 was more important for the Guangzhou and Shanghai sites mainly owing to their high NO_x levels. And the O_3 production at the Lanzhou site seemed to be less sensitive to all of these processes due to its relatively low concentrations of aerosol and NO_x. These findings indicate the varying impacts of

heterogeneous processes on the O_3 photochemistry in different regions of China, and suggest further necessity to better understand these processes.

(4) In summary, the results of this study have provided insights into O_3 pollution, local chemistry versus outside impact, and potential impacts of heterogeneous chemistry in major urban areas of China. The high-quality data taken in the mid-2000s will be particularly valuable for assessing the atmospheric impact of rapid urbanization/industrialization process in China.

Acknowledgement

The authors are grateful to Steven Poon, Waishing Wu and Jiamin Zhang for their contributions to the field work, and to Drs. Tijian Wang and Jie Tang for their help in selecting the study sites. We would like to thank the Master Chemical Mechanism group in University of Leeds for providing the mechanism. We also appreciate two anonymous reviewers who raised helpful comments to improve our manuscript. The field measurements were funded by the Research Grants Council of Hong Kong (HKRGC; PolyU5144/04E), and the data analysis were supported by the Hong Kong Polytechnic University (1-BB94 and 1-ZV9N) and the HKRGC (PolyU5015/12P).

References

Aldener, M., Brown, S., Stark, H., Williams, E., Lerner, B., Kuster, W., Goldan, P., Quinn, P., Bates, T., and Fehsenfeld, F.: Reactivity and loss mechanisms of NO_3 and N_2O_5 in a polluted marine environment: Results from in situ measurements during New England Air Quality Study 2002, *J. Geophys. Res.*, 111, D23S73, doi: 10.1029/2006JD007252, 2006.

Aumont, B., Chervier, F., and Laval, S.: Contribution of HONO sources to the $NO_x/HO_x/O_3$ chemistry in the polluted boundary layer, *Atmos. Environ.*, 37, 487–498, 2003.

Berlin, S. R., Langford, A. O., Estes, M., Dong, M., and Parrish, D. D.: Magnitude, decadal changes, and impact of regional background ozone transported into the greater Houston, Texas Area, Environ. Sci. Tech., 47, 13985-13992, 2013.

Brown, S. S., Ryerson, T. B., Wollny, A. G., Brock, C. A., Peltier, R., Sullivan, A. P., Weber, R. J., Dube, W. P., Trainer, M., Meagher, J. F., Fehsenfeld, F. C., and Ravishankara, A. R.: Variability in nocturnal nitrogen oxide processing and its role in regional air quality, *Science*, 311, 67-70, 2006.

Cardelino, C. A., and Chameides, W. L.: An Observation-Based Model for Analyzing Ozone Precursor Relationships in the Urban Atmosphere, *J. Air Waste Manage*, 45, 161-180, 1995.

Chang, W. L., Bhave, P. V., Brown, S. S., Riemer, N., Stutz, J., and Dabdub, D.: Heterogeneous Atmospheric Chemistry, Ambient Measurements, and Model Calculations of N_2O_5: A Review, *Aerosol Sci Tech.*, 45, 665-695, 2011.

Chou, C. C. K., Tsai, C. Y., Chang, C. C., Lin, P. H., Liu, S. C., and Zhu, T.: Photochemical production of ozone in Beijing during the 2008 Olympic Games, *Atmos. Chem. Phys*., 11, 9825-9837, 2011.

Ding, A. J., Fu, C. B., Yang, X. Q., Sun, J. N., Zheng, L. F., Xie, Y. N., Hermann, E., Nie, W., Petaja, T., Kerminen, V.-M., and Kulmala, M.: Ozone and fine particle in the western Yangtze River Delta: an overview of 1-yr data at the SORPES station, *Atmos. Chem. Phys.*, 13, 5813-5830, 2013.

Ding, A. J., Wang, T., Thouret, V., Cammas, J. P., and Nedelec, P.: Tropospheric ozone climatology over Beijing: analysis of aircraft data from the MOZAIC program, *Atmos. Chem. Phys*., 8, 1-13, 2008.

Frost, G. J., Trainer, M., Allwine, G., et al.: Photochemical ozone production in the rural southeastern United States during the 1990 Rural Oxidants in the Southern Environment (ROSE) progarm, *J. Geophys. Res.-Atmos.*, 103, D17, 22491-22508, 1998.

Gao, J., Wang, T., Zhou, X. H., Wu, W. S., and Wang, W. X.: Measurement of aerosol number size distributions in the Yangtze River delta in China: Formation and growth of particles under polluted conditions, *Atmos. Environ.*, 43, 829-836, 2009.

George, C., Strekowski, R., Kleffmann, J., Stemmler, K., and Ammann, M.: Photoenhanced uptake of gaseous NO_2 on solid organic compounds: a photochemical source of HONO?, *Faraday Discuss*., 130, 195-210, 2005.

Jacob, D. J.: Introduction to Atmospheric Chemistry, Princeton University Press, New Jersey, 1999.

Jenkin, M. E., Saunders, S. M., Wagner, V., and Pilling, M. J.: Protocol for the development of the Master Chemical Mechanism, MCM v3 (Part B): tropospheric degradation of aromatic volatile organic compounds, *Atmos. Chem. Phys*., 3, 181-193, 2003.

Kanaya, Y., Pochanart, P., Liu, Y., Li, J., Tanimoto, H., Kato, S., Suthawaree, J., Inomata, S., Taketani, F., Okuzawa, K., Kawamura, K., Akimoto, H., and Wang, Z. F.: Rates and regimes of photochemical ozone production over Central East China in June 2006: a box model analysis using comprehensive measurements of ozone precursors, *Atmos. Chem. Phys*., 9, 7711-7723, 2009.

Li, G., Lei, W., Zavala, M., Volkamer, R., Dusanter, S., Stevens, P., and Molina, L. T.: Impacts of HONO sources on the photochemistry in Mexico City during the MCMA-2006/MILAGO Campaign, *Atmos. Chem. Phys*., 10, 6551-6567, 2010.

Liu, Z., Wang, Y., Gu, D., Zhao, C., Huey, L. G., Stickel, R., Liao, J., Shao, M., Zhu, T., Zeng, L., Amoroso, A., Costabile, F., Chang, C. C., and Liu, S. C.: Summertime photochemistry during CAREBeijing-2007: RO_x budgets and O_3 formation, *Atmos. Chem. Phys*., 12, 7737-7752, 2012.

Mao, J., Jacob, D. J., Evans, M. J., Olson, J. R., Ren, X., Brune, W. H., St Clair, J. M., Crounse, J. D., Spencer, K. M., Beaver, M. R., Wennberg, P. O., Cubison, M. J., Jimenez, J. L., Fried, A., Weibring, P., Walega, J. G., Hall, S. R., Weinheimer, A. J., Cohen, R. C., Chen, G., Crawford, J. H., McNaughton, C., Clarke, A. D., Jaegle, L., Fisher, J. A., Yantosca, R. M., Le Sager, P., and Carouge, C.: Chemistry of hydrogen oxide radicals (HO_x) in the Arctic troposphere in spring, *Atmos. Chem. Phys*., 10, 5823-5838, 2010.

Monge, M. E., D'Anna, B., Mazri, L., Giroir-Fendler, A., Ammann, M., Donaldson, D. J., and George, C.: Light changes theatmospheric reactivity of soot, *Proc. Natl. Acad. Sci.*, 107, 6605–6609, 2010.

Molina, M. J., and Molina, L. T.: Megacities and atmospheric pollution, *J. Air Waste Manage.*, 54, 644-680, 2004.

Mozurkewich, M., McMurry, P. H., Gupta, A., and Calvert, J. G.: Mass accommodation coefficient of HO_2 on aqueous particles, *J. Geophys. Res.*, 92(D4), 4163-4170, 1987.

Ohara, T., Akimoto, H., Kurokawa, J., Horii, N., Yamaji, K., Yan, X., and Hayasaka, T.: An Asian emission inventory of anthropogenic emission sources for the period 1980-2020, *Atmos. Chem. Phys*., 7, 4419-4444, 2007.

Parrish, D. D., and Zhu, T.: Clean Air for Megacities, *Science*, 326, 674-675, 2009.

Pathak, R. K., Wu, W. S., and Wang, T.: Summertime $PM_{2.5}$ ionic species in four major cities of China: nitrate formation in an ammonia-deficient atmosphere, *Atmos. Chem. Phys*., 9, 1711-1722, 2009.

Ran, L., Zhao, C. S., Geng, F. H., Tie, X. X., Tang, X., Peng, L., Zhou, G. Q., Yu, Q., Xu, J. M., and Guenther, A.: Ozone photochemical production in urban Shanghai, China: Analysis based on ground level observations, *J. Geophys. Res.-Atmos.*, 114, 2009.

Ryerson, T. B., Trainer, M., Angevine, W. M., Brock, C. A., Dissly, R. W., Fehsenfeld, F. C., Frost,

G. J., Goldan, P. D., Holloway, J. S., Hubler, G., Jakoubek, R. O., Kuster, W. C., Neuman, J. A., Nicks Jr., D. K., Parrish, D. D., Roberts, J. M., and Sueper, D. T.: Effect of petrochemical industrial emissions of reactive alkenes and NOx on tropospheric ozone formation in Houston, Texas, *J. Geophys, Res.-Atmos.*, 108(D8), 4249, 2003.

Saunders, S. M., Jenkin, M. E., Derwent, R. G., and Pilling, M. J.: Protocol for the development of the Master Chemical Mechanism, MCM v3 (Part A): tropospheric degradation of non-aromatic volatile organic compounds, *Atmos. Chem. Phys*., 3, 161-180, 2003.

Stockwell, W. R., Lawson, C. V., Saunders, E., and Goliff, W. S.: A review of tropospheric atmospheric chemistry and gas-phase chemical mechanisms for air quality modeling, *Atmosphere*, 3, 1-32, 2012.

Su, H., Cheng, Y. F., Shao, M., Gao, D. F., Yu, Z. Y., Zeng, L. M., Slanina, J., Zhang, Y. H., and Wiedensohler, A.: Nitrous acid (HONO) and its daytime sources at a rural site during the 2004 PRIDE-PRD experiment in China, *J. Geophys, Res.-Atmos.*, 113, 2008.

Su, H., Cheng, Y. F., Oswald, R., Behrendt, T., Trebs, I., Meixner, F. X., Andreae, M. O., Cheng, P., Zhang, Y., and Poschl, U.: Soil Nitrite as a Source of Atmospheric HONO and OH Radicals, *Science*, 333, 1616-1618, 2011.

Taketani, F., Kanaya, Y., Pochanart, P., Liu, Y., Li, J., Okuzawa, K., Kawamura, K., Wang, Z., and Akimoto, H.: Measurement of overall uptake coefficients for HO_2 radicals by aerosol particles sampled from ambient air at Mts. Tai and Mang (China), *Atmos. Chem. Phys*., 12, 11907-11916, 2012.

Thornton, J. A., Jaegle, L., and McNeill, V. F.: Assessing known pathways for HO_2 loss in aqueous atmospheric aerosols: Regional and global impacts on tropospheric oxidants, *J. Geophys, Res.-Atmos.*, 113, 2008.

Tie, X., Geng, F., Guenther, A., Cao, J., Greenberg, J., Zhang, R., Apel, E., Li, G., Weinheimer, A., Chen, J., and Cai, C.: Megacity impacts on regional ozone formation: observations andWRF-Chem modeling for the MIRAGE-Shanghai field campaign, *Atmos. Chem. Phys.*, 13, 5655–5669, 2013.

Vogel, B., Vogel, H., Kleffmann, J., and Kurtenbach, R.: Measuredand simulated vertical profiles of nitrous acid - Part II. Modelsimulations and indications for a photolytic source, *Atmos. Environ.*, 37, 2957–2966, 2003.

Wang, T., Ding, A. J., Gao, J., and Wu, W. S.: Strong ozone production in urban plumes from Beijing, China, *Geophys. Res. Lett.*, 33, 2006.

Wang, T., Wei, X. L., Ding, A. J., Poon, C. N., Lam, K. S., Li, Y. S., Chan, L. Y., and Anson, M.: Increasing surface ozone concentrations in the background atmosphere of Southern China, 1994-2007, *Atmos. Chem. Phys*., 9, 6216-6226, 2009b.

Wang, T., Nie, W., Gao, J., Xue, L. K., Gao, X. M., Wang, X. F., Qiu, J., Poon, C. N., Meinardi, S., Blake, D., Wang, S. L., Ding, A. J., Chai, F. H., Zhang, Q. Z., and Wang, W. X.: Air quality during the 2008 Beijing Olympics: secondary pollutants and regional impact, *Atmos. Chem. Phys*.,10, 7603-7615, 2010b.

Wang, X., Zhang, Y., Hu, Y., Zhou, W., Lu, K., Zhong, L., Zeng, L., Shao, M., Hu, M., and Russell, A. G.: Process analysis and sensitivity study of regional ozone formation over the Pearl River Delta, China, during the PRIDE-PRD2004 campaign using the Community Multiscale Air Quality modeling system, *Atmos. Chem. Phys*., 10, 4423-4437, 2010c.

Xu, X., Lin, W., Wang, T., Yan, P., Tang, J., Meng, Z., and Wang, Y.: Long-term trend of surface ozone at a regional background station in eastern China 1991-2006: enhanced variability, *Atmos. Chem. Phys*., 8, 2595-2607, 2008.

Xue, L. K., Wang, T., Zhang, J. M., Zhang, X. C., Deliger, Poon, C. N., Ding, A. J., Zhou, X. H., Wu, W. S., Tang, J., Zhang, Q. Z., and Wang, W. X.: Source of surface ozone and reactive nitrogen speciation at Mount Waliguan in western China: New insights from the 2006 summer study, *J. Geophys, Res.-Atmos.*, 116, 2011.

Xue, L. K., Wang, T., Guo, H., Blake, D. R., Tang, J., Zhang, X. C., Saunders, S. M., and Wang, W. X.: Sources and photochemistry of volatile organic compounds in the remote atmosphere of western China: results from the Mt. Waliguan Observatory, *Atmos. Chem. Phys*.,13, 8551-8567, 2013.

Xue, L. K., Wang, T., Louie, P. K. K., Luk, C. W. Y., Blake, D. R., and Xu, Z.: Increasing external effects negate local efforts to control ozone air pollution: a case study of Hong Kong and implications for other Chinese cities, *Environ. Sci. Tech.*, 48 (18), 10769-10775, 2014a.

Xue, L. K., Wang, T., Wang, X. F., Blake, D. R., Gao, J., Nie, W., Gao, R., Gao, X. M., Xu, Z., Ding, A. J., Huang, Y., Lee, S. C., Chen, Y. Z., Wang, S. L., Chai, F. H., Zhang, Q. Z., and Wang, W. X.: On the use of an explicit chemical mechanism to dissect peroxy acetyl nitrate formation, *Environ.*

Pollution, 195, 39-47, 2014b.

Zhang, J., Wang, T., Chameides, W. L., Cardelino, C., Kwok, J., Blake, D. R., Ding, A., and So, K. L.: Ozone production and hydrocarbon reactivity in Hong Kong, Southern China, *Atmos. Chem. Phys*., 7, 557-573, 2007.

Zhang, J. M., Wang, T., Ding, A. J., Zhou, X. H., Xue, L. K., Poon, C. N., Wu, W. S., Gao, J., Zuo, H. C., Chen, J. M., Zhang, X. C., and Fan, S. J.: Continuous measurement of peroxyacetyl nitrate (PAN) in suburban and remote areas of western China, *Atmos. Environ.*, 43, 228-237, 2009a.

Zhang, L., Chen, C. H., Li, S. X., and Zhang, F.: Air pollution and potential control schemes in Lanzhou, *Res. Environ. Sci*., 13, 18-21, 2000.

Zhang, L., Brook, J. R., and Vet, R.: A revised parameterization for gaseous dry deposition in air-quality models, *Atmos. Chem. Phys*., 3, 2067-2082, 2003.

Zhang Q., Yuan B., Shao M., Wang, X., Lu, S., Lu, K., Wang, M., Chen, L., Chang, C., and Liu S.: Variations of ground-level O_3 and its precursors in Beijing in summertime between 2005 and 2011, *Atmos. Chem. Phys.*, 14, 6089-6101, 2014.

Zhang, Q., Streets, D. G., Carmichael, G. R., He, K. B., Huo, H., Kannari, A., Klimont, Z., Park, I. S., Reddy, S., Fu, J. S., Chen, D., Duan, L., Lei, Y., Wang, L. T., and Yao, Z. L.: Asian emissions in 2006 for the NASA INTEX-B mission, *Atmos. Chem. Phys*., 9, 5131-5153, 2009b.

Zhang, Y. H., Su, H., Zhong, L. J., Cheng, Y. F., Zeng, L. M., Wang, X. S., Xiang, Y. R., Wang, J. L., Gao, D. F., Shao, M., Fan, S. J., and Liu, S. C.: Regional ozone pollution and observation-based approach for analyzing ozone-precursor relationship during the PRIDE-PRD2004 campaign, *Atmos. Environ.*, 42, 6203-6218, 2008.

Table 1. Overview of ozone pollution conditions in four Chinese cities.

Site	Location	Observation Period	Number of O_3 episode days[a]	Maximum hourly O_3 (ppbv)
Beijing *CP*	116.30 °E, 40.35 °N	June 21 – July 31 2005	18	286
Shanghai *Taicang*	121.10 °E, 31.45 °N	May 4 – June 1 2005	6	127
Guangzhou *WQS*	113.55 °E, 22.70 °N	April 20 – May 26 2004	7	178
Lanzhou *RSP*	103.69 °E, 36.13 °N	June 19 – July 16 2006	8	143

[a]The ozone episode day is defined here as the one with the maximum hourly ozone exceeding 100 ppbv.

Figure Captions:

Fig. 1. Map showing the study areas and anthropogenic NO_x emissions over China. The emission data was obtained from Zhang et al. (2009b).

Fig. 2. Observed average diurnal profiles of (a) NO_y and (b) CO in the four cities. The data time interval is 10 minutes, and the error bar is standard error.

Fig. 3. Average OH reactivities of major hydrocarbons at the four cities. The error bar is standard error.

Fig. 4. O_3 accumulation and contributions from *in-situ* chemistry, regional transport, and deposition during episodes in (a) Beijing (9 July 2005), (b) Shanghai (7 May 2005), (c) Guangzhou (24 May 2004), and (d) Lanzhou (11 July 2006). Note that the blue bars are added to the red ones.

Fig. 5. The OBM-calculated RIRs for (a) major O_3 precursor groups and (b) the AHC sub-groups during high O_3 events in Shanghai, Guangzhou and Lanzhou.

Fig. 6. Average increase in the daytime-average O_3 production rates by including $ClNO_2$ formation (ϕ_{ClNO2}=0.6) during episodes at four cities. Also shown are the model-simulated nighttime $ClNO_2$ concentrations and the product of NO_2 with aerosol surface. The error bars are standard deviations. The number in parentheses gives the increase in percentage.

Fig. 7. Average reductions in the daytime-average HO_2 concentrations and O_3 production rates by adjusting γ_{HO2} from 0.02 to 0.4 during episodes at four cities. Also shown are the observed aerosol surface area concentrations (note that the data in Guangzhou was inferred from the measurements at a nearby station in Hong Kong). The error bars are standard deviations.

Fig. 8. Average increase in the daytime-average O_3 production rate by including HONO formation from heterogeneous NO_2 reactions during episodes at four cities. Also shown are the modeled daytime-average HONO concentrations. The error bars are standard deviations. The number in parentheses gives the increase in percentage.

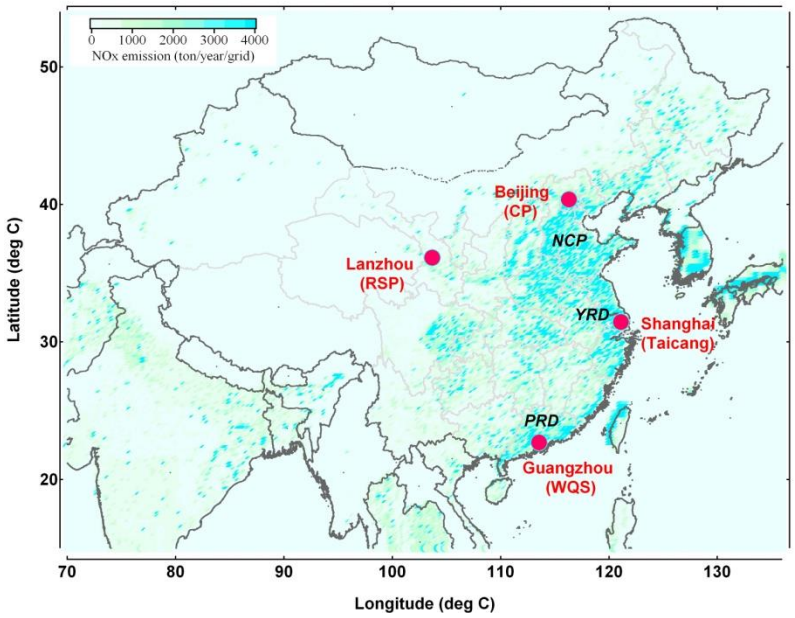
0 1000 2000 3000 4000
NOx emission (ton/year/grid)
Beijing
(CP)
NCP
Lanzhou
(RSP)
YRD
Shanghai
(Taicang)
PRD
Guangzhou
(WQS)
Latitude (deg C)
Longitude (deg C)
50
40
30
20
70
80
90
100
110
120
130

Fig. 1

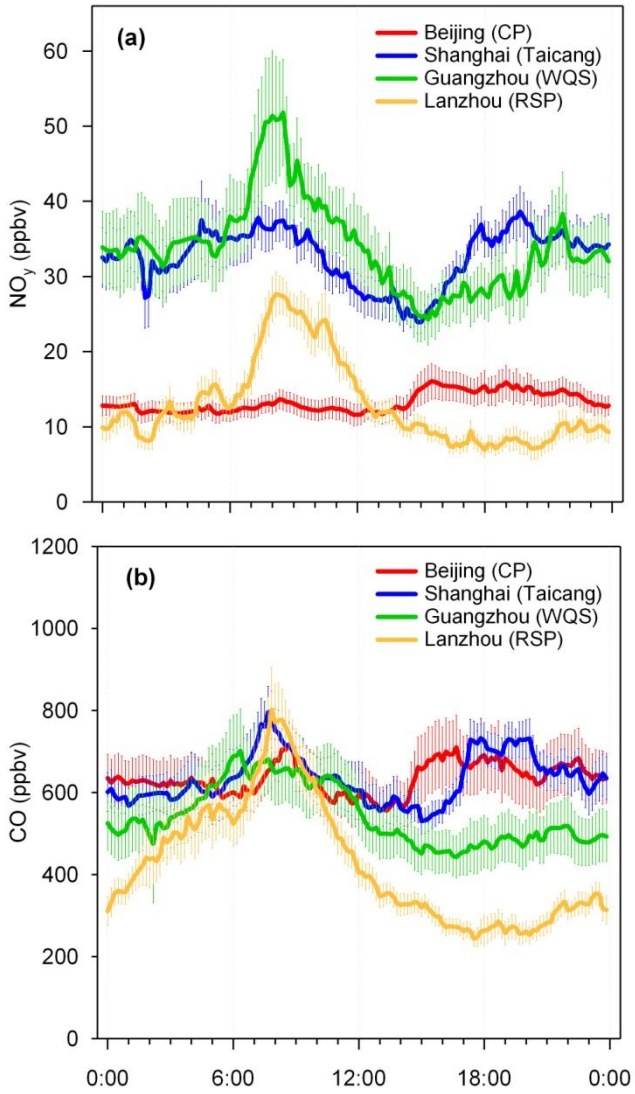
(a)
Beijing (CP)
Shanghai (Taicang)
Guangzhou (WQS)
Lanzhou (RSP)
NOy (ppbv)
0
10
20
30
40
50
60
(b)
Beijing (CP)
Shanghai (Taicang)
Guangzhou (WQS)
Lanzhou (RSP)
CO (ppbv)
0
200
400
600
800
1000
1200
0:00
6:00
12:00
18:00
0:00

Fig. 2

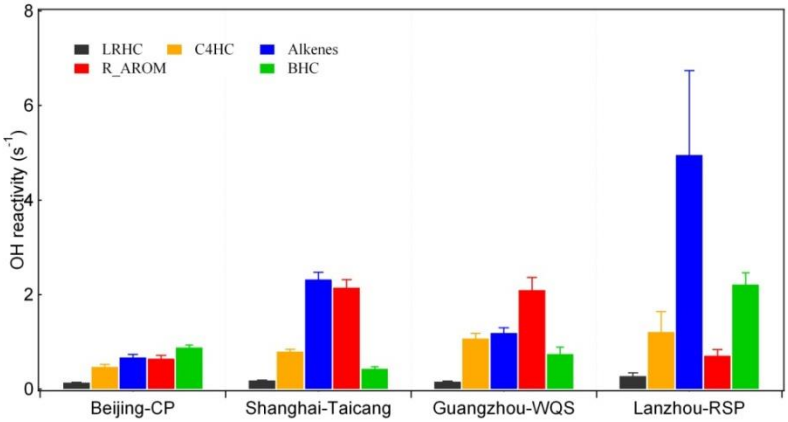
LRHC
C4HC
Alkenes
R_AROM
BHC
OH reactivity (s-1)
0
2
4
6
8
Beijing-CP
Shanghai-Taicang
Guangzhou-WQS
Lanzhou-RSP

Fig. 3

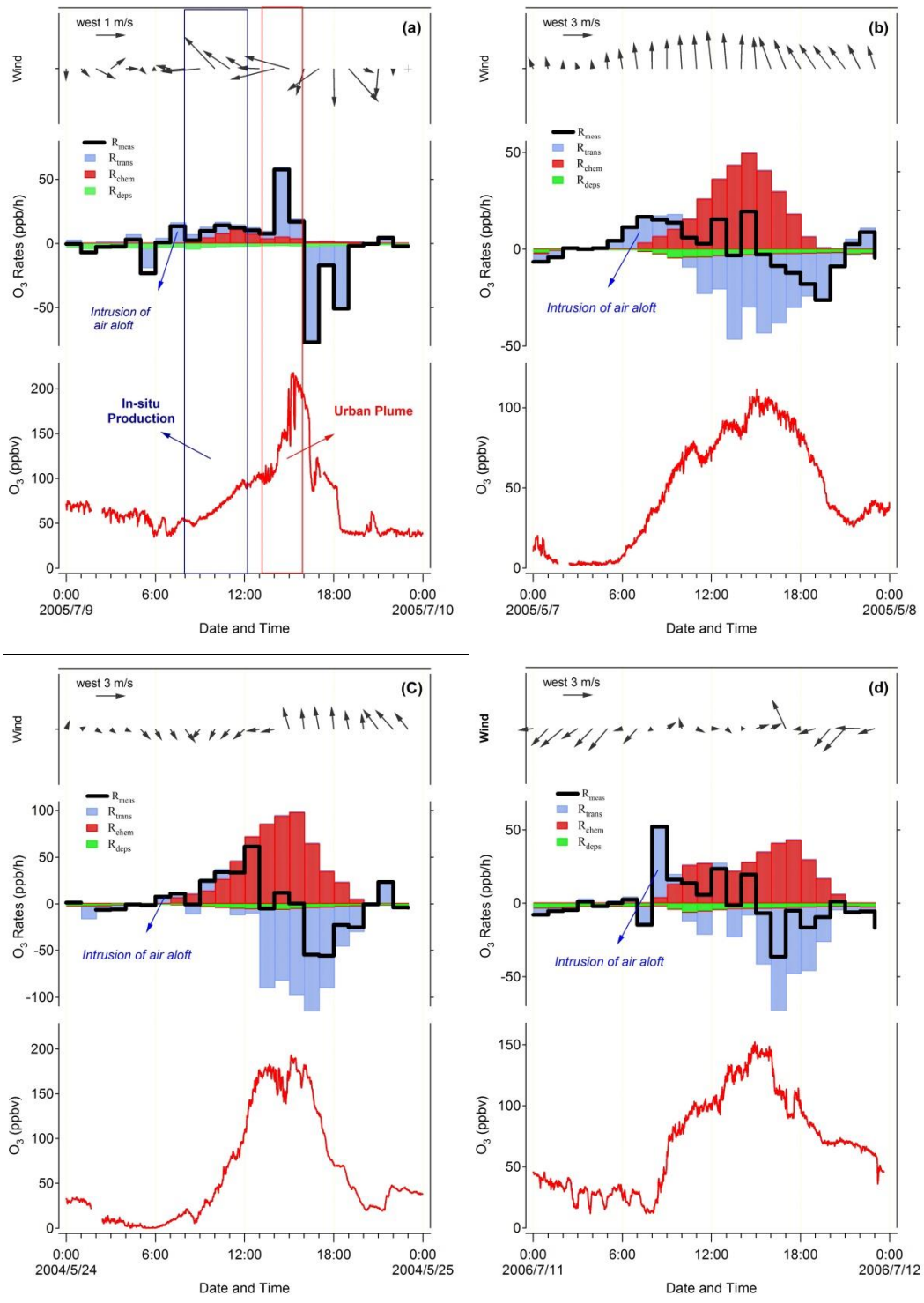
(a)
west 1 m/s
Wind
R_{meas}
R_{trans}
R_{chem}
R_{deps}
O_3 Rates (ppb/h)
Intrusion of air aloft
In-situ Production
Urban Plume
O_3 (ppbv)
0:00 2005/7/9
6:00
12:00
18:00
0:00 2005/7/10
Date and Time
(b)
west 3 m/s
Intrusion of air aloft
0:00 2005/5/7
0:00 2005/5/8
(C)
west 3 m/s
Intrusion of air aloft
0:00 2004/5/24
0:00 2004/5/25
(d)
west 3 m/s
Intrusion of air aloft
0:00 2006/7/11
0:00 2006/7/12

Fig. 4

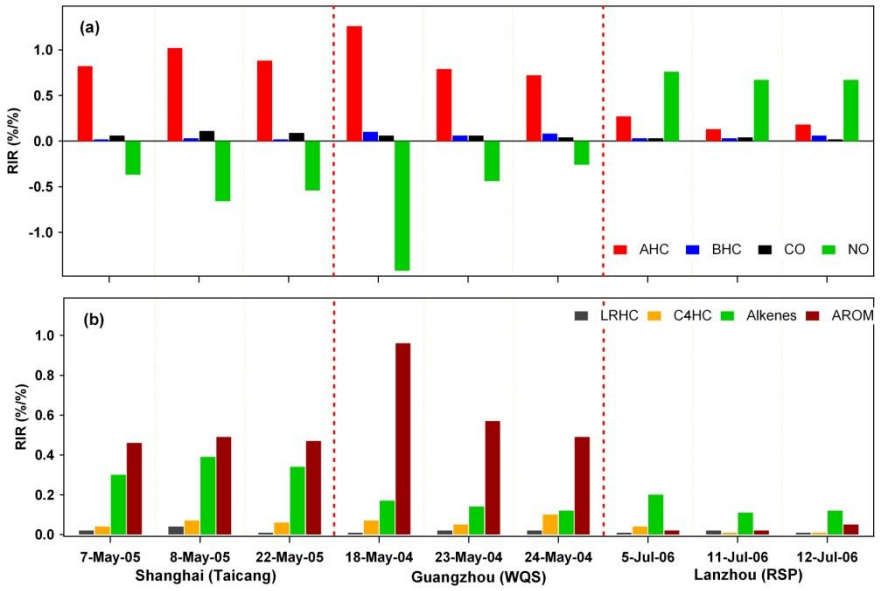
(a)
RIR (%/%)
1.0
0.5
0.0
-0.5
-1.0
AHC
BHC
CO
NO
(b)
LRHC
C4HC
Alkenes
AROM
RIR (%/%)
1.0
0.8
0.6
0.4
0.2
0.0
7-May-05
8-May-05
22-May-05
Shanghai (Taicang)
18-May-04
23-May-04
24-May-04
Guangzhou (WQS)
5-Jul-06
11-Jul-06
12-Jul-06
Lanzhou (RSP)

Fig. 5

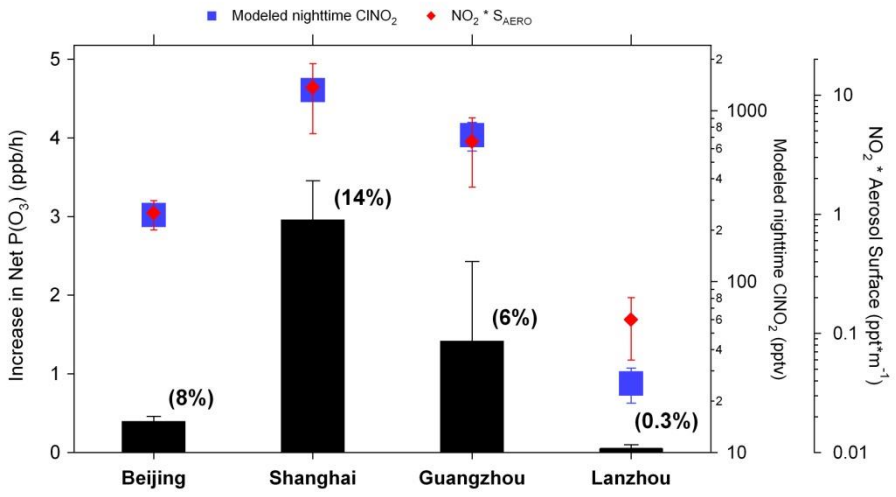
Modeled nighttime ClNO2
NO2 * SAERO
Increase in Net P(O3) (ppb/h)
5
4
3
2
1
0
(8%)
(14%)
(6%)
(0.3%)
Beijing
Shanghai
Guangzhou
Lanzhou
Modeled nighttime ClNO2 (pptv)
1000
100
10
NO2 * Aerosol Surface (ppt*m-1)
10
1
0.1
0.01

Fig. 6

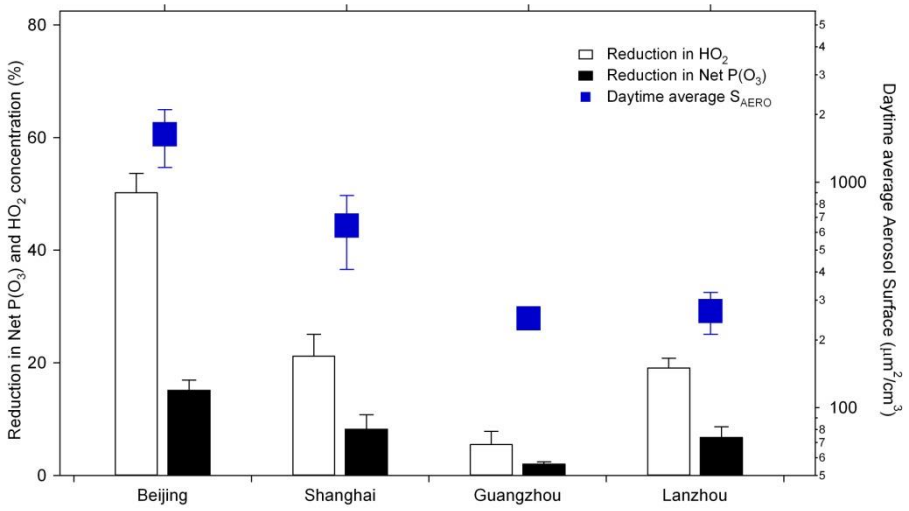
Reduction in HO2
Reduction in Net P(O3)
Daytime average SAERO
Reduction in Net P(O3) and HO2 concentration (%)
Daytime average Aerosol Surface (μm2/cm3)
Beijing
Shanghai
Guangzhou
Lanzhou

Fig.7

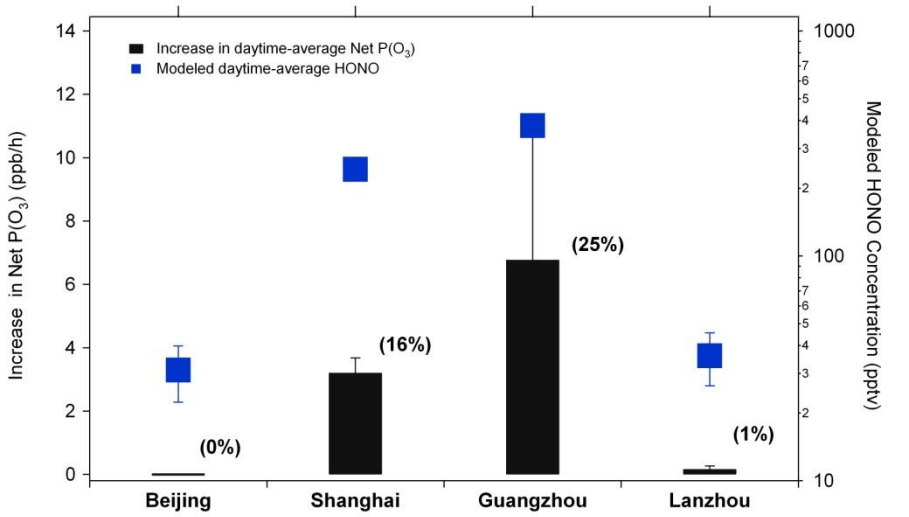
Increase in daytime-average Net P(O3)
Modeled daytime-average HONO
Increase in Net P(O3) (ppb/h)
Modeled HONO Concentration (pptv)
(0%)
(16%)
(25%)
(1%)
Beijing
Shanghai
Guangzhou
Lanzhou

Fig. 8